Environmental Science and Pollution Research (2024) 31:34258–34270
https://doi.org/10.1007/s11356-024-33539-9

RESEARCH ARTICLE

Co-composting of green waste and biogas waste: physical, chemical parameters and quality of ripe compound

Mauricio Aparecido Bortoloti[1] · Adriana Zemiani Challiol[1] · Isabela Mangerino Bortoloti Sicchieri[1] · Emília Kiyomi Kuroda[1] · Fernando Fernandes[1]

Received: 13 September 2023 / Accepted: 28 April 2024 / Published online: 3 May 2024

Abstract

The impact of adding biogas waste (BW) to green waste (GW) composting to increase nitrogen supplementation and improve mature compost quality was investigated. Conducted over 90 days using static windrows, the experiment compared treatments with GW alone (T1) and GW supplemented with BW (T2 and T3). The results showed that the addition of BW increased temperatures, improved the C/N ratio, and expedited the stabilization process compared to T1. Furthermore, the addition of BW led to significant degradation of hemicellulose (up to 39.98%) and cellulose (up to 27.63%) compared to GW alone. Analysis of Fourier-transform infrared (FTIR) spectra revealed the presence of aromatic, phenolic, aliphatic, and polysaccharide structures in the compost, with BW supplementation enhancing these characteristics. Importantly, the germination index (GI) assessment indicated that the compounds produced were not toxic and instead exhibited stimulatory effects on seed germination. Overall, the findings suggest that supplementing GW composting with BW can enhance the quality and efficacy of the composting process, resulting in compost with desirable properties for agricultural use.

Keywords Structuring substrate · Nutrients · Stabilization · Fertilizer · Phytotoxicity · Lignin

Introduction

Biological processes are widely used for the recovery of organic waste. Around the world, organic waste processing units are increasingly present in discussions about clean and renewable energy sources (Pang et al. 2021).

The concept of the circular economy suggests the use of technologies that enhance the use of waste as inputs for common use, where the exploitation and contamination of natural resources are minimized by the cycle of use. Composting, an emerging circular economy approach, amplifies the process and improves compost quality by incorporating and eliminating the waste stream, which in turn increases nutrient recycling through microbial activity (Ofei-Quartey et al. 2023).

Composting, in turn, consists of the biotransformation of organic matter by microorganisms and related enzymes, which convert organic residues into stable and complex macromolecules. The final product is a nutritious compound from an agronomic perspective, usable in agricultural crops, and can be an alternative to chemical fertilization (He et al. 2022).

Organic waste with less potential for biodegradation, such as green waste (GW) derived from tree and grass pruning, is generally used in composting processes as a structuring material. As they contain a high percentage of lignocellulosic material, they are difficult to metabolize, making their application in anaerobic digestion (AD) processes challenging.

Responsible Editor: Ta Yeong Wu

✉ Mauricio Aparecido Bortoloti
mauricio.bortoloti@uel.br

Adriana Zemiani Challiol
adrianazemiani@gmail.com

Isabela Mangerino Bortoloti Sicchieri
isabela.sicchieri@uel.br

Emília Kiyomi Kuroda
ekkuroda@uel.br

Fernando Fernandes
fernando@uel.com.br

[1] Department of Civil Engineering, Center for Technology and Urbanism, State University of Londrina, Celso Garcia Cid Highway (PR-445), Km 380, Londrina, Paraná 86057-970, Brazil

Even in the composting process, GW presents difficulties in biodegradation and delays in stabilization due to its chemical characteristics. With high concentrations of lignocellulose, nitrogen deficit, and consequent low C/N ratio (Meng et al. 2019), the process becomes slow, and the final product is deficient in nutrients (dal Bosco 2017). Recent studies show that the use of lignocellulosic residues associated with biogas waste (BW) in the composting process brings benefits to the stabilization and quality of both residues, reducing BW ammonia concentrations, and increasing nitrogen and ammonium nitrate levels in the final compost (Li et al. 2020; Zhong et al. 2021).

The effluent from the AD process, or BW, is considered an interesting soil conditioner and agricultural biofertilizer (Dutta et al. 2021). However, BW derived from short methanization processes may not be stabilized, presenting a high organic load and high concentrations of ammonia. Unstable BW should be used with reservations due to the volume produced and environmental problems that can arise, such as leaching of toxic compounds, unpleasant odors, pathogens, and phytotoxins (Meng et al. 2020; Sheng et al. 2022; Xu et al. 2022).

The total stabilization of biogas residue occurring inside the anaerobic reactor prolongs the hydraulic retention time (HRT), which increases the demand for reactor volume to process the same volume of residues. Thus, stabilization in composting processes becomes interesting for BW, allowing for the reduction of reactor dimensions and consequently minimizing the costs of implementing the system, in addition to avoiding environmental impacts resulting from the inadequate disposal of waste (Pramanik et al. 2019; Meng et al. 2019; Bai et al. 2020).

The co-composting of structuring residues and BW is essential due to the reduced granulometry of BW, preventing the formation of anaerobic zones (Meng et al. 2019). Additionally, benefits observed in other studies include increased C/N ratio, process temperature, shorter compost stabilization time, higher material degradation rate, and nutritional improvement of the final compost (Tambone et al. 2015; Bai et al. 2020; Meng et al. 2020).

Various structuring substrates have already been reported in the literature, such as rice straw and food residues (Bai et al. 2020); residue from the industrialization of mushrooms; and residues from swine breeding (Meng et al. 2019), rice straw, and swine manure (Zhong et al. 2021), associated with BW of reactors fed with rice straw, corn residues, and rice straw and swine manure, respectively. Therefore, the use of GW associated with BW of a reactor that treats food waste is proposed in this study as a suggestion for the combination of co-substrates.

In this study, waste with reckless disposal was transformed into compost applicable for improving soil quality, emphasizing the concept of the circular economy and closing the material cycle. To this end, the effects of adding RV on RV composting time of trees and grass clippings generated in small volumes were evaluated. The physical and chemical parameters were monitored during the process, and the stabilization and interaction between them were used to evaluate maturation. In addition, the toxicity of the produced compounds was evaluated by means of a germination test at three composting periods. Finally, these values were related to assessing the maturity and quality of the compounds.

Materials and methods

Collection and characterization of substrates

The residues used in the composting windrows were collected on the campus of Universidade Estadual de Londrina (UEL), Paraná, Brazil. The GW consisted of tree branch pruning (TP) and grass pruning (GP). The TP was obtained after pruning the Azalea bush (*Rhododendron simsii*) and tree species such as Ingá Feijão (*Inga cylindrica*), Flamboyant (*Delonix regia*), and Santa Bárbara (*Melia azedarach*). The GPs were collected after mowing.

The BW corresponds to the sedimented fraction of the effluent after 48 h at rest. It was collected from the bottom of the effluent tank of a continuous stirred-tank reactor (CSTR), which treats food waste, with an HRT of 40 days, an average volumetric organic load (OLR) of 0.72 kgVS m^{-3} day^{-1}, and biogas production of 0.63 m^3 $kgVS^{-1}$, as reported in the study conducted by Bortoloti et al. (2023). The residues were characterized physicochemically (Table 1) following the analyses of the American Public Health Association (APHA 2017).

Table 1 Physicochemical characterization of substrates used in the composting test

Parameter	Unity	TP	GP	BW
pH	-	5.72	5.42	8.64
EC	μs cm^{-1}	719	685	11.960
TS	g kg^{-1}	693.1	881.5	47.5*
VTS	g kg^{-1}	648.1	819.3	35.0*
FTS	g kg^{-1}	44.9	62.2	12.4*
Umidity content	%	30.69	11.84	95.25
Density	kg L^{-1}	0.100	0.039	1.005
Carbon, C	g kg^{-1}	360.0	455.1	19.4*
Nitrogen, N	g kg^{-1}	5.1	8.3	9.4*
C/N ratio	-	71	54	2
Sodium	mg kg^{-1}	-	-	403.70

TP, tree pruning; *GP*, grass pruning; *BW*, biogas waste

* values given in g L^{-1}

Composting

The TPs were mechanically crushed into pieces smaller than 20 cm. A preliminary quantitative study of the waste generated within the limits of the University campus of UEL was carried out to determine the treatments tested, as follows: mixture only of GW proportional to the respective generation between TP and GP (T1); mixing the proportions of GW with the addition of BW in the proportions of generation between the sources of waste (T2); and the third condition (T3) considering a C/N ratio of 30.

The windrows were assembled in layers of approximately 10 cm, interspersing the constituent substrates, to ensure better mixing (Table 2). In T2, 5 L of water was added to the layers that did not receive BW. The BW added to each layer was proportional to the number of layers and the amount in each treatment. After finishing the layers, all the windrows received a GP coverage, which was considered in the sum of the total mass of the windrows (Table 2).

The windrows were set up in a trapezoidal format with dimensions of 2.4 m × 1.2 m ($W \times B$). The height of the windrows varied according to the treatment composition. The treatments that received the addition of BW showed a lower height, due to the liquid characteristic of the substrate. Thus, the heights were 60, 55, and 50 cm for treatments T1, T2, and T3, respectively. It is noteworthy that the experiment was conducted in an area with a roof and a waterproofed floor.

The dynamics of analyses and monitoring carried out throughout the study are shown in Fig. 1; however, the analyses carried out before the windrows were assembled and after completion are not presented.

Physicochemical analyses

For daily temperature measurement, a digital thermometer with a metal rod (Jenco Model 701) was used in three positions in the vertical section of the windrows (right side, center, and left side). To obtain the horizontal temperature profile, three points of the same depth were used. The sum of these points corresponds to the average temperature of each treatment.

The ambient, maximum, and minimum temperatures at the experiment location were obtained daily at the time of measuring the temperatures of the windrows using an HTC-1 thermometer.

The determination of the percentages of total solids (TS), volatile total solids (VS), fixed total solids (FS),

Table 2 Composition of treatments in the composting experiment

Treatment	Substrates	Mix ratio (kg:kg:kg)	C/N ratio	Bulk (m^3)	Added mass (kg)	Corrected umidity (%)
T1	TP + GP	2.5:1	65	1.4	109.8	57
T2	TP + GP + BW	1.8:0.7:1	43	1.6	175.4	58
T3	TP + GP + BW	0.9:0.35:1	30	1.2	173.2	62

TP, tree pruning; *GP*, grass pruning; *BW*, biogas waste

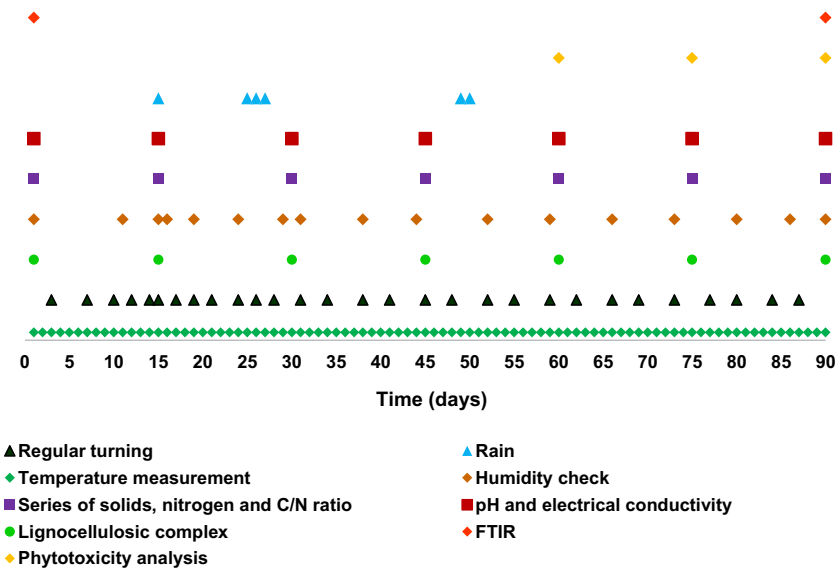

Fig. 1 Chronological events and activities carried out in the composting experiment

and moisture was performed weekly using the gravimetric method (APHA 2017). The value of organic carbon was quantified fortnightly by dividing the value of VS by the factor 1.8 (Jimnez and Garcia 1992).

The pH and electrical conductivity (EC) of the samples were measured fortnightly using a soluble stratum (SE), produced with 10 g of sample in 100 mL of deionized water. The mixture was stirred for 30 min on a shaker table at 100 rpm. The samples were kept at rest for 60 min, and then the supernatant was submitted for analysis (Tedesco et al. 1995). Nitrogen analysis was performed by the Micro-Kjeldhal method (APHA 2017) using a Digester Block and Buchi Distiller.

The aeration of the windrows was maintained by manual turning, with the frequency of turnings varying between two and three times a week.

Lignocellulosic complex

To determine the lignocellulosic complex (lignin, cellulose, and hemicellulose), the method for determining the fibrous components of lignocellulosic residues proposed by Van Soest (1964) was used. This method is based on the use of detergents and reagents that result in the separation and quantification of the different constituent fractions of the material, and its use has been well established (Hindrichsen et al. 2006; Farias et al. 2015; Carvalho et al. 2021).

In summary, the dried and ground compost was packed into TNT (non-woven fabric) packages and subjected to baths in neutral detergents (FDN) and acid detergents (FDA) in autoclaves under internal environmental conditions of 105 °C for 60 min, washed with water, and dried in a forced-air oven until constant weight. Based on the dry mass values, the FDN (hemicellulose) and FDA (cellulose) contents were calculated (Eq. 1).

$$\text{FDN or FDA}(\%) = \frac{(package\ weight + waste) - (empty\ package\ weight)}{\text{sample weight (in dry matter)}} * 100 \quad (1)$$

For lignin, the packages are immersed in a solution of H2SO4 (72%) for 3 h (Eq. 2). Subsequently, the packages were washed and dried in a forced air oven at 60 °C until constant weight.

$$\text{Lignin}\ (\%) = \frac{(package\ weight + waste) - (ash\ weight)}{\text{sample weight(in dry matter)}} * 100 \quad (2)$$

The ash content was calculated after the samples were calcined in a muffle furnace at 500 °C for 4 h.

Attenuated total reflectance–Fourier transform infrared spectroscopy (ATR-FTIR)

Infrared spectra were generated using a Frontier FTIR spectrophotometer (PerkinElmer, USA) equipped with a diamond crystal attenuated total reflectance accessory and zinc selenide support. Samples from different composting times, dried and finely ground, were prepared by adding three drops of glycerin, using the same material as the background spectrum. A small amount of each sample was deposited onto the crystal, and a torque of 20 N was applied with an articulated arm. The spectra were acquired at a resolution of 4 cm^{-1} by averaging 32 scans in the wave number range from 550 to 4000 cm^{-1}.

Phytotoxicity analysis

To verify the toxicity of the compounds obtained at 60, 75, and 90 days of conducting the experiment, an assay was carried out to verify the germination index (GI), widely accepted for the evaluation of the compounds produced. For this, an SE of the treatments was produced in the proportion of 1:10 (m:v) of compost and deionized water (Tiquia et al. 1996; Huang et al. 2016). The mixture was kept in orbital agitation at 150 rpm for 24 h. The supernatant was centrifuged at 1200 rpm for 20 min, filtered through a 1.2-µm cellulose ester microfilter, using a vacuum filtration system. The filtrate was frozen at – 10 °C until used.

For sowing, two sheets of Germitest paper were used under 9-cm diameter Petri dishes. Ten milliliters of filtered SE was added onto the leaves, where 10 seeds of *Lipidium sativum* (garden cress) were arranged on each plate. SE was tested at 100% concentration. For the control, deionized water was used. All conditions tested were performed in triplicate.

After sowing, the treatments remained incubated at 25 °C (± 1 °C) and in the absence of light for 72 h (Zeng et al. 2017). Means of counting the germinated seeds and measuring the length of the roots: The number of germinated seeds was considered to calculate the seed germination rate (SGR) and the germination index (GI) through Eqs. (3) and (4) (Zucconi et al. 1981).

$$SGR = \frac{ANGS * 100\%}{NSP} \quad (3)$$

$$GI = \frac{ANGS * ALR * 100\%}{ANGSC * ALRC} \quad (4)$$

ANGS average number of germinated seeds;

NSP number of seeds per plate;

ALR average length of root;

ANGSC average number of germinated seeds in the control;

ALRC average length of root in control.

The results were subjected to statistical analysis using the R Software. With the guarantee of the model's assumptions, normality of residues, and homogeneity of variance, the means of the analyzed treatments were compared to verify the toxicity or not of the compounds. To verify the influence of the composting time on the final compost with ES at 100%, the factorial analysis was carried out in a 3 × 3 arrangement with the parameters treatment (swaths) and composting time, for SGR and GI.

Results and discussion

Physicochemical parameters

Temperature

Temperature is a primary indicator of efficiency in the composting process, closely linked to the speed of organic material degradation and the growth of microorganisms and their communities (Meng et al. 2020). Throughout the experiment, the temperature exhibited different behaviors in the treatments (Fig. 2).

The temperatures for treatments T2 and T3 rose relatively slowly, reaching peak temperatures after day 8 of processing. These results are similar to those reported by Meng et al. (2019), who, using BW from corn AD mixed with residue from mushroom production and swine manure, observed temperatures above 50 °C only around the 10th day. In contrast, Bai et al. (2020) observed temperatures around 50 °C on the first day of processing BW from rice straw, food leftovers, cattle manure, and raw rice straw.

T1 exhibited a slower temperature rise rate than the other treatments, with peak temperatures observed only after 30 days of the process. This was attributed to the high C/N ratio at the beginning of the process. As T1 did not receive the addition of BW, the nitrogen concentration was very low, resulting in an initial C/N ratio of 65, which is considerably higher than the optimal C/N ratio of 30 for the effective development of the composting process (Fourti 2013; dal Bosco 2017; Bai et al. 2020; Meng et al. 2020).

El Ouaqoudi et al. (2015) suggested that the difficulty in raising temperatures in processes involving lignocellulosic materials is related to the high lignin content and its distribution in cells, which can hinder biological activity and act as physical or chemical barriers to the decomposition of cellulose and other carbohydrates.

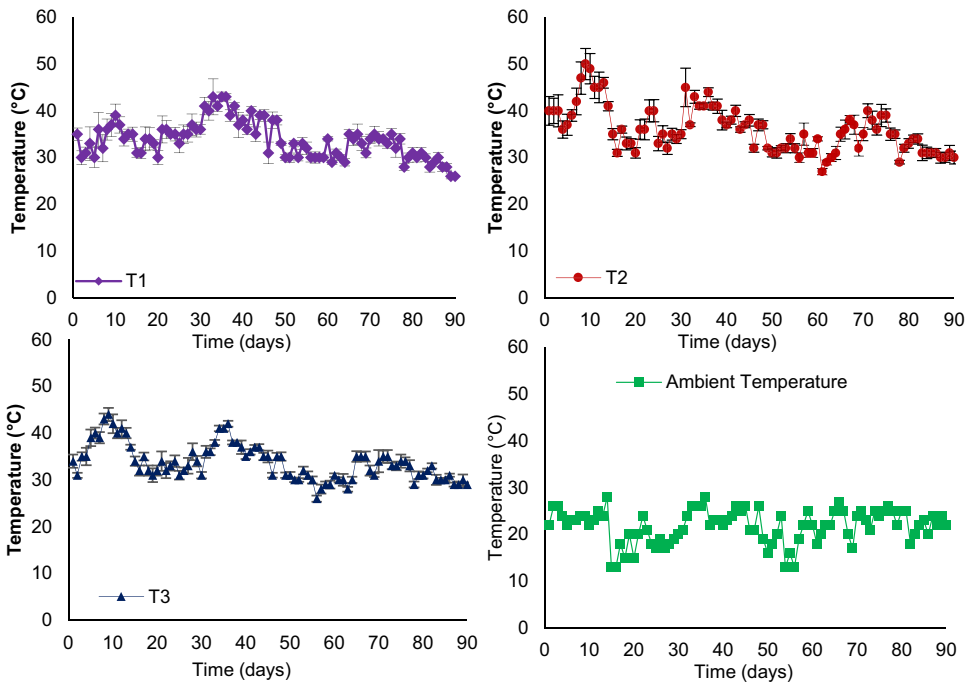

Fig. 2 Average temperature verified in the process for the treatments studied. T1 (TP + GP – 2.5:1); T2 (TP + GP + BW – 1.8:0.7:1); T3 (TP + GP + BW – 0.9:0.6:1)

The size of the windrows may have affected the heating dynamics, as windrows smaller than 1 m^3 may lack thermal inertia (Kiehl 1985). Temperatures exceeding 55 °C are essential for compost sanitization and proper process development, resulting in stable and moist compost (dal Bosco 2017).

Despite their reduced dimensions, the windrows experienced periods of low temperatures, approximately 5 °C at the beginning of processing, when temperatures should ideally rise to their peak levels. In contrast to the current study, Sun et al. (2017) managed to maintain temperatures above 50 °C even in low ambient temperatures around 10 °C by inoculating the process with microorganisms adapted to the prevailing temperature.

Although lower than expected, the process temperature tends to continue, albeit at a slower pace in stabilizing the material (dal Bosco 2017). Treatments T2 and T3 reached average temperatures above 40 °C (thermophilic phase) only after the 8th day of monitoring, lasting for 3 days for T3 and 5 days for T2, which according to Meng et al. (2019) is sufficient time for compost sanitization.

The highest temperature observed, 50 °C in T2 on the 9th day of monitoring, was below the expected values. Veras et al. (2020), comparing static and aerated windrow systems, reported temperatures of 64 °C and 59 °C, respectively.

As the process progressed, compost temperature tended to decrease, indicating compound maturation. This decrease in temperature is considered an indicator of compound maturation by Meng et al. (2020). dal Bosco (2017) noted that the temperature drop is associated with reduced biological activity due to the depletion of available organic material for metabolism. The treatments began to exhibit temperatures close to room temperature after 50 days of monitoring, indicating the initiation of compound maturation.

Electric conductivity

The pH of the composting process must be maintained at values close to neutrality to ensure adequate conditions for microbiological activity (Maragno et al. 2007). For all treatments, the pH values remained stable, remaining close to neutrality (Fig. 3).

After the initiation of the process, treatments 2 and 3 exhibited a gradual reduction in pH up to 45 days. Treatment 1, however, showed a reduction in pH only at 45 days. Meng et al. (2020) attribute the decrease in pH values to intense microbiological activity. In this study, treatment 1 presented a nutritional deficit due to the absence of BW, resulting in lower microbiological activity.

After 60 days of processing, the pH values began to increase again. At the end of the stabilization phase, acids formed through protein synthesis decompose, generating ammonia (NH4 +), which raises the pH value of the process. Such an occurrence is mentioned by Meng et al. (2020), who report the increase in pH as an indication of the stabilization of organic matter and the initiation of compound mineralization.

Ho et al. (2022) highlight the observed dynamics of pH reduction, elevation, and stabilization as typical of the composting process, attributing these changes to variations in the chemical composition of the mixtures during the process.

Regarding electrical conductivity (EC), similar effects were observed. Treatments 2 and 3 presented higher ion concentrations compared to treatment 1, which did not receive BW addition. Despite BW being the result of sedimentation of the AD effluent, some residual salts from the anaerobic process remained in the sludge mass used, influencing the EC of the treatments, as reported by Bustamante et al. (2008), Silva et al. (2009), and Akyol et al. (2019).

Decreases in EC values were observed at the beginning of the process, with values reduced to 489 µS cm^{-1}, 680 µS

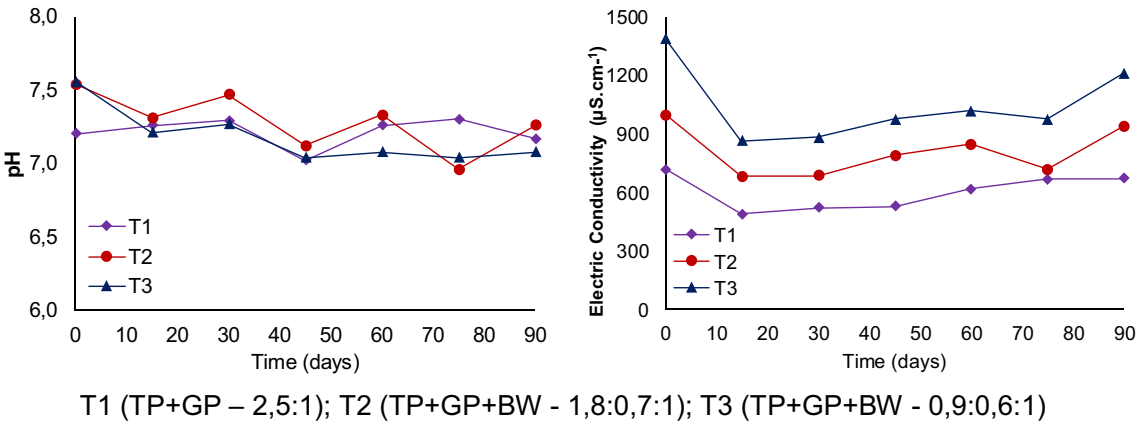

Fig. 3 Variation of pH and EC for the treatments studied. T1 (TP + GP – 2.5:1); T2 (TP + GP + BW – 1.8:0.7:1); T3 (TP + GP + BW – 0.9:0.6:1)

cm^{-1}, and 862 µS cm^{-1} for treatments 1, 2, and 3, respectively, on day 45 of monitoring. This reduction was likely due to the addition of water to maintain windrow humidity, which could have led to the leaching of some salt ions. Ammonia volatilization and precipitation of mineral salts are also factors that can contribute to a decrease in EC (Meng et al. 2020).

After day 45 of monitoring, EC values increased, indicating the decomposition of organic matter and mineralization of the compost, resulting in a higher concentration of salts and an increase in EC levels (Tambone et al. 2015; Meng et al. 2019). From this point until the end of the experiment, EC values for treatments 2 and 3 continued to increase, reaching values of 939 µS cm^{-1} and 1210 µS cm^{-1}, respectively, by the end of the process.

Treatment 1 exhibited an increase in EC only on the 90th day, indicating that the reduction in carbon concentration was delayed due to the high initial C/N ratio. The influence of BW on EC values can be observed, with treatment 3, which had the highest BW addition, showing the highest parameter values. The sodium concentration in BW proportionally increased the EC values, albeit remaining below 4000 µS cm^{-1}, considered the maximum EC limit (Meng et al. 2019). Values greater than 2500 µS cm^{-1} are sufficient to inhibit the growth of plants and microorganisms (Meng et al. 2020).

Carbon, nitrogen, and C/N ratio

In composting, the most assimilated carbon (C) is consumed by microorganisms and excreted in the form of CO_2, while the recalcitrant C products of lignocellulosic materials are humified (Meng et al. 2020). Green wastes (GW) are rich in recalcitrant C; therefore, they require longer processing time to be stabilized. Thus, the C/N ratio is a parameter that exhibits gradual and constant changes.

The carbon corrections (Fig. 4) showed a decrease at the end of the 90-day composting period compared to the initial values. The reduction in carbon is linked to the degradation of organic matter and the reduction of microbiological activity during aerobic degradation (Vig et al. 2011). Similar to known foods, variations in organic concentration are indicative of biological activity. After 45 days of processing, it was observed that the material was reduced, and the fluctuation period was similar to that indicated by Meng et al. (2020), who observed stabilization of the C concentration after 30 days.

Total nitrogen (TN) is fundamental in the process, aiding in the synthesis of microbial cells, which ensures the reproduction of organisms at rates compatible with the process requirements (Meng et al. 2020). TN deficiency implies a reduction in microbial replication and a consequent increase in processing time (dal Bosco 2017).

During the composting process, part of the TN derived from the substrates is metabolized and assimilated by microorganisms for cellular synthesis, while part is released in the form of NH_3, N_2, and NOx. The largest portion of TN is fixed in the humus through microbial mineralization in the form of nitrate (Meng et al. 2020).

The addition of BW to treatments T2 and T3 increased the concentration of nutrients, enabling an improvement in the C/N ratio of these treatments. With initial ratios of

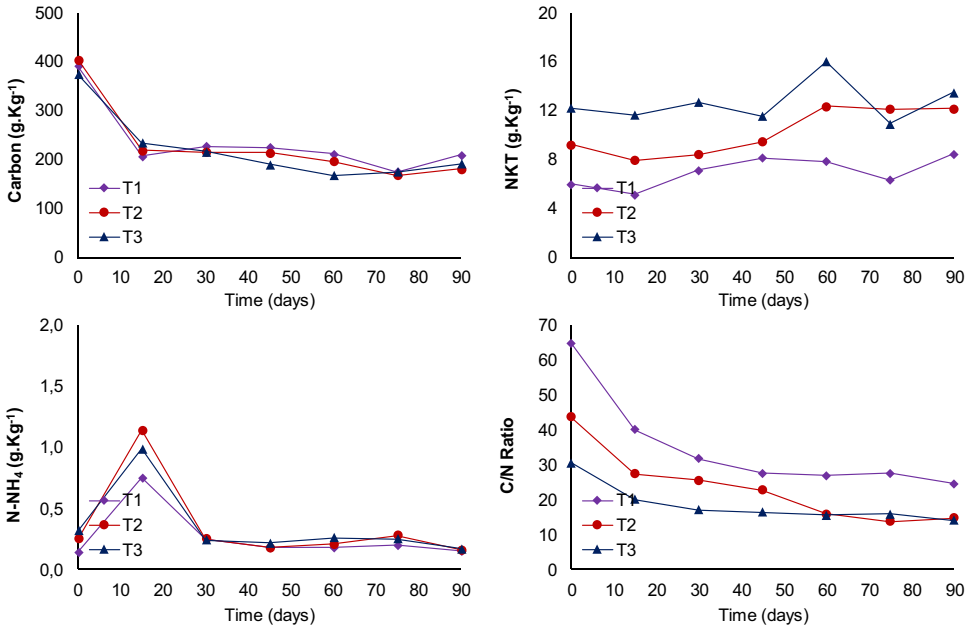

Fig. 4 Variation of carbon, nitrogen, and total ammonia and C/N ratio for the treatments studied. T1 (TP + GP – 2.5:1); T2 (TP + GP + BW – 1.8:0.7:1); T3 (TP + GP + BW – 0.9:0.6:1)

9.3 g kg^{-1} and 12.2 g kg^{-1} for T2 and T3, respectively, the greater supply of TN for these treatments resulted in an overall improvement of the parameters.

In all tested treatments, there was an increase in concentrations throughout the process. The increases observed in TN concentrations for all treatments, according to Kiehl (1985), are related to the mineralization of organic matter, as reported by Chikae et al. (2006).

Nitrogen (N) is related to the pH values of the process. Nitrogen losses can occur at pH above 9.5 due to the conversion of ammonium ion (NH_4^+) into ammonia. For the present study, the highest pH value observed was 8.13, in T3 on the 3rd day of monitoring. Thus, it is suggested that ammonia volatilization was low. If the pH rises above the indicated levels, Zhang et al. (2013) suggest adjusting the parameters to reduce ammonia volatilization, aiding in retaining nutrients in the compost.

The concentrations of ammoniacal nitrogen (NH_4–N) varied throughout the monitoring period, with the highest values identified at 30 days of the process. The increases observed in NH_4–N concentrations may be related to the release of free ammonia (NH_3). Zhang et al. (2013) mention that the release of NH_3 may be associated with the increase in pH. Thus, the observed increase in pH at 45 days into the process led to a reduction in the concentration of ammoniacal nitrogen, as reported by Jumnoodoo and Mohee (2011). They suggest that high pH values inhibit microbiological activity, reducing NH_4–N absorption and resulting in ammonia volatilization. Zhang et al. (2013) also mention reductions in the pH of the composting process and suggest that this was due to ammonium ion volatilization in the windrows, as observed in the present study.

It is recommended that the composting process starts with a C/N ratio close to 30. Fourti (2013) states that if the C/N ratio deviates from the optimal range, composting progresses slowly. Excess carbon is converted into CO_2, or excess nitrogen is converted into ammonia, until the correct balance is restored, slowing down degradation and increasing the time required for stabilization of the process.

Treatment 1 had the highest initial C/N ratio at 65. High C/N ratio values can inhibit microbial activity due to nitrogen deficiency, which, at low concentrations, inhibits the microbiological activity responsible for synthesizing proteins (Meng et al. 2020). Treatment 2 had a C/N ratio of 43, a value above the recommended range, but with a greater supply of TN compared to treatment 1, allowing for better conditions for microbial activity, although still above the ideal level. After the beginning of the process, microbiological activity degraded the most volatile fraction of organic matter, reducing the percentages of volatile solids (VS) and, consequently, carbon contents.

At the end of the process, the final C/N ratios for the treatments were 24, 14, and 14 for T1, T2, and T3, respectively. dal Bosco (2017) consider C/N ratio values close to 10 indicative of process stability, and for all treatments, the C/N ratio stabilized above the indicated range.

Lignin, cellulose, and hemicellulose

During the compost processing period, the percentages of cellulose and hemicellulose decreased continuously, showing a tendency to stabilize after 60 days (Fig. 5), consistent with the findings of Bai et al. (2020), Liu et al. (2017), and Wang et al. (2017).

Among the constituent compounds of lignocellulose, hemicellulose is the most easily biodegradable fraction, serving as a source of carbon and energy for microorganisms involved in the process (Bai et al. 2020). The decline in the degradation curve of cellulose and hemicellulose is more pronounced at the beginning of the process, coinciding with higher temperatures during the thermophilic phase. This suggests that hemicellulose was the primary lignocellulosic compound actively degraded during this phase (Liu et al. 2017), while the degradation of cellulose was relatively slower.

Bai et al. (2020) observed a similar reduction in hemicellulose percentages in the initial days, attributing it to high temperatures and biological activity. In our study, the percentages of hemicellulose at the start of the process were 26.26% ± 3.84, 29.97% ± 0.76, and 25.28% ± 0.41 for T1, T2, and T3, respectively. By the end of the processing, these percentages decreased to 19.23% ± 0.37, 17.99% ± 1.31, and 18.45% ± 1.37 for T1, T2, and T3, respectively, representing reductions of 26.76%, 39.98%, and 27.01%, respectively.

The variation in cellulose percentage became more evident after 15 days of processing, coinciding with the thermophilic phase onset for treatments T2 and T3. Liu et al. (2017) attribute this dynamic heating to the thermal decomposition of compounds in progress. Cellulose content in treatments T2 and T3 began decreasing later in the composting process, becoming more noticeable between days 30 and 45, mainly due to lignin degradation, albeit mitigated by inhibitory effects (Bai et al. 2020). The percentages of cellulose at the start of the process were 33.26% ± 0.18, 33.94% ± 1.63, and 32.65% ± 0.89 for T1, T2, and T3, respectively, ending at 28.83% ± 5.17, 24.56% ± 0.80, and 24.90% ± 1.01 for T1, T2, and T3, respectively, representing reductions of approximately 13.32%, 27.63%, and 23.75%, respectively.

As a more resistant lignocellulosic constituent (Meng et al. 2019), lignin percentages increased by day 30 compared to the start of the process, then showed reductions before stabilizing by the end of the process. Relative lignin content at the beginning of the process was 21.10% ± 1.10, 22.82% ± 2.00, and 20.93% ± 0.15 for T1, T2, and T3, respectively, increasing to 35.75% ± 3.94, 32.67% ± 1.46, and 34.23% ± 0.67, respectively, by the end of the process,

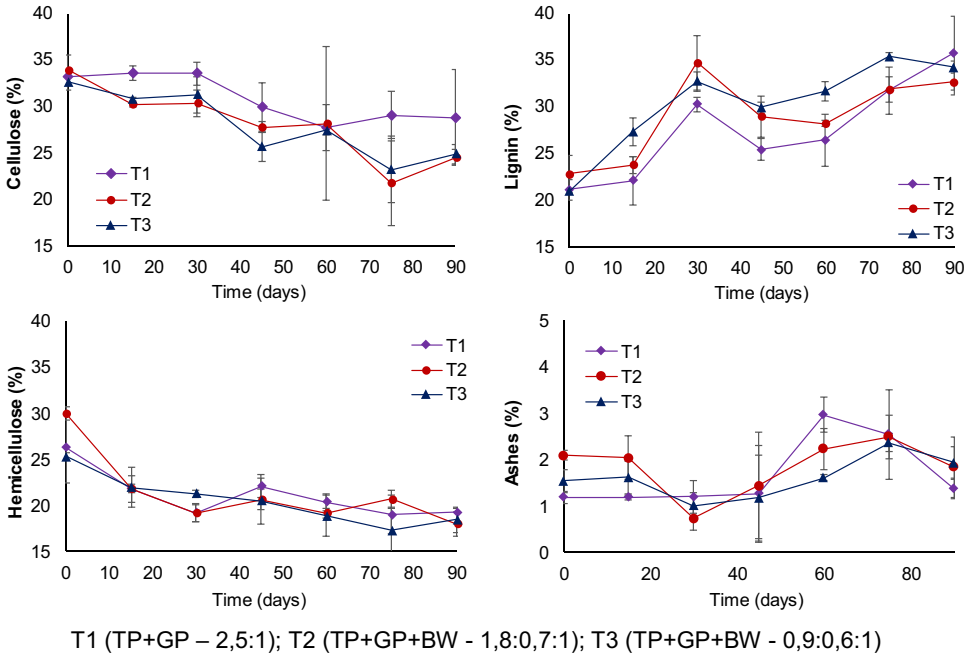

Fig. 5 Variation of the lignocellulosic complex for the treatments studied. T1 (TP + GP – 2.5:1); T2 (TP + GP + BW – 1.8:0.7:1); T3 (TP + GP + BW – 0.9:0.6:1)

representing increases of 69.43%, 43.14%, and 63.54%, respectively.

Bai et al. (2020) attribute the increase in lignin content to synergistic interactions of microbial communities and biodegradable organic matter, which declined faster than lignin. Despite the treatments showing reductions in dry matter of approximately 28.3%, 27.8%, and 32.3% for T1, T2, and T3, respectively, implying an increase in lignin percentage, this was obscured by the reduction in the amount of dry mass processed.

Liu et al. (2017) explain that while the relative content of lignin increased, the absolute content decreased, albeit at a slower rate than cellulose and hemicellulose. Therefore, they suggest considering only cellulose and hemicellulose as indicative of lignocellulosic material degradation. Regarding absolute content, considering the identified mass reduction, the increases in lignin were approximately 21.15%, 3.25%, and 9.57% for T1, T2, and T3, respectively. Despite the percentage increases, there appears to be differentiation between treatments, suggesting that T2 exhibited more degradation of lignocellulosic compounds.

Analysis of Fourier transform infrared spectroscopy—FTIR

Infrared spectroscopy analyses were employed to identify the presence and variations of functional groups in samples from the three treatments under consideration (Fig. 6). The main peaks observed were located at 1042, 1637, 2913, and 3319 cm^{-1}. Zhu et al. (2021) attribute the bands from 1000 to 1150 cm^{-1} to the stretching of C–O in alcohols, ethers, and polysaccharide esters. Bands near 1655 cm^{-1} are related to the stretching of CO in amide I and ketones, which are present in the decomposition of proteins and polysaccharides (Yu et al. 2019).

The 1042 cm^{-1} band is attributed to variations in the concentration of polysaccharides and carbohydrates (Yang et al. 2019). Initially in the composting process, the reduction is attributed to high biological activity and the consequent increase in temperature. Toward the end of the process, with mature compost, changes in this relationship are attributed to the concentration of carboxylate ions and alkyl carbon after the degradation of more biodegradable organic matter. This is also related to the reduction of carboxylate ions and metabolized sugars in the formation of humic substances.

The typical lignin peak can be observed in the range of 1408–1525 cm^{-1}, as evidenced in this study at 1424 and 1637 cm^{-1}, resulting from the symmetric C–H bonding of aliphatic components, characterizing the CH3 group in lignin (El Ouaqoudi et al. 2015; Wu et al. 2022). Peaks identified within the 1870–1540 cm^{-1} range are associated with the axial deformation of C = O (carboxylic acids, ketones, and aldehydes), referring to hemicellulose-based compounds. Kong et al. (2023) emphasize that peaks around 1600 cm^{-1} are associated with the gradual decomposition of proteins and sugars during the composting process, forming aromatic substances and later humus. These substances are related to process stability, and humus is beneficial for agriculture.

Variations in the ratio between the 1637 and 2913 cm^{-1} bands (aromatic C = C/aliphatic C–H) are attributed to increased aromaticity, carboxylate concentration, and

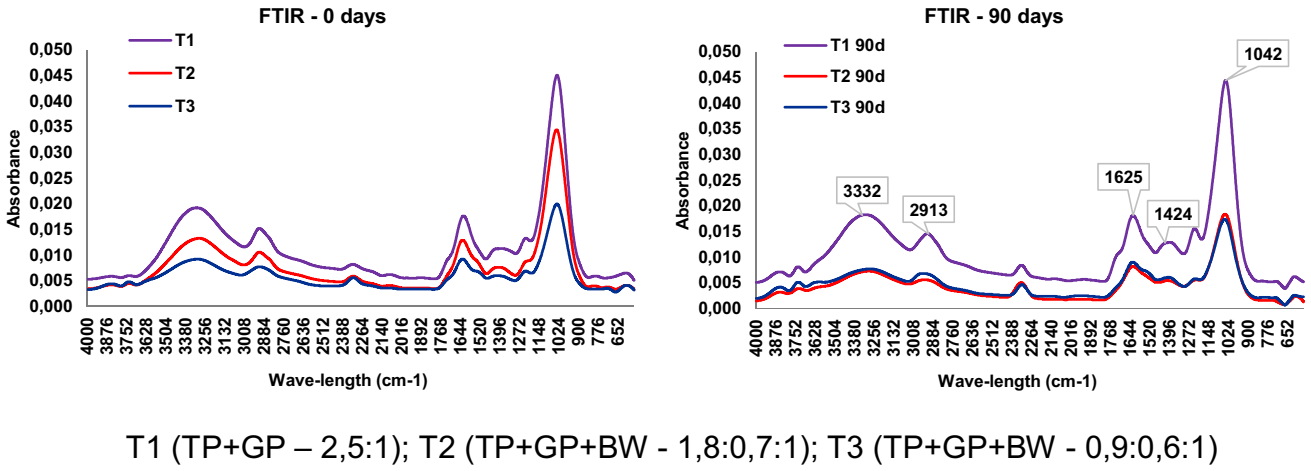

Fig. 6 FTIR spectrum for the treatments studied over the course of monitoring. T1 (TP + GP – 2.5:1); T2 (TP + GP + BW – 1.8:0.7:1); T3 (TP + GP + BW – 0.9:0.6:1)

reduced polysaccharides in the compounds (El Ouaqoudi et al. 2015). This indicates that organic matter becomes more complex during composting as processing stabilizes and matures the material (Som et al. 2009). The peak around 2913 is associated with the stretching of C–H in aliphatic structures (Amir et al. 2010), and the decrease in this peak indicates the degradation of aliphatic compounds and carbohydrates, such as cellulose, hemicellulose, and lignin (Zhang et al. 2023).

Bands in the 3000–2800 cm^{-1} range are attributed to the hydrophobic properties of organic material and are related to methyl and methylene aliphatic groups. Characteristic aliphatic C–H bands tend to decrease in intensity during the co-composting process, consistent with the microbial oxidation of aliphatic and peptidic compound chains, providing information about the degradation of organic material during the composting process (El Fels et al. 2014).

Wu et al. (2022) attribute the band at 3340.71 cm^{-1} to the axial vibration of OH stretching of phenols and alcohols, identified in this study at 3332 cm^{-1}. The reduction in the intensity of this band is attributed to the decomposition of aliphatic carbon during the composting process, indicating a reduction in the availability of organic matter to be stabilized. According to Rueda et al. (2023), bands near the 3300 cm^{-1} region are related to the stretching of hydroxyl OH groups, linked to carboxylic acids, alcohols, and phenols, and are also associated with the stretching of N–H bonds.

Phytotoxicity test

The treatment factors, processing time, and their respective interactions showed no significant effect on SGR or GI at the 5% significance level (p-value > 0.05) (Table 3). The factorial statistical analysis of variance indicated that there is no significant difference between the interactions of the variation factors and the treatments tested. Therefore, it is considered that none of the treatments exhibited toxicity. Consequently, the compounds generated in the treatments after 60 days, under all the conditions tested, could be used for agriculture without causing toxic effects on plant germination. The mean values of the triplicates for each treatment, as well as the standard deviation (SD), for SGR and GI are presented in Table 4.

The highest percentage of seed germination rate (TGS) was observed for T2 at 60 days (86.67%), along with the highest germination index (GI) (148.99%). GI values higher

Table 3 Results of analysis of variance by 3 × 3 factorial arrangement comparing treatments and processing times for SGR and GI

Variation	Factor SGR				
	DF	SS	MS	Fc	p-value
Treatment	3	121.1	40.351	0.367	0.777
Time	2	3.7	1.852	0.016	0.983
Treatment:time	4	596.3	149.07	1.356	0.263
Residual	47	5166.7	109.92		
Total	56	5.8777			
	Factor GI				
Treatment	3	1.549	516.22	0.803	0.498
Time	2	844	422.16	0.657	0.522
Treatment:time	4	1.744	436.02	0.678	0.610
Residual	47	30.189	642.32		
Total	56	34.326			

DF, degrees of freedom; *SS*, sum of squares; *MS*, medium square; *Fc*, calculated *F* value; *SGR*, seed germination rate; *GI*, germination index

Table 4 Mean results and standard deviation of the phytotoxicity test for SGR and GI and the factor analysis of the results, considering the condition and processing time factors

Treatment	Monitoring times (days)	% of SE	SGR (%)		GI (%)	
Control	-	DW	80.00 ± 10.00	Aa	100.00 ± 23.93	Aa
T1	60	100	80.00 ± 10.00	Aa	119.03 ± 20.74	Aa
T2			8667 ± 5.77	Aa	148.99 ± 20.04	Aa
T3			63.33 ± 5.77	Aa	116.74 ± 20.21	Aa
T1	75		86.67 ± 5.77	Aa	126.71 ± 4.08	Aa
T2			70.00 ± 10.00	Aa	107.00 ± 23.32	Aa
T3			80.00 ± 10.00	Aa	133.57 ± 14.70	Aa
T1	90		76.67 ± 11.55	Aa	121.50 ± 13.70	Aa
T2			66.67 ± 5.77	Aa	112.43 ± 25.93	Aa
T3			73.33 ± 15.28	Aa	112.23 ± 25.93	Aa

Capital letters refer to the "treatment" factor; lowercase letters refer to the "processing time" factor. T1 (TP + GP – 2.5:1); T2 (TP + GP + BW – 1.8:0.7:1); T3 (TP + GP + BW – 0.9:0.6:1); *SL*, soluble layer; *DW*, deionized water; *SGR*, seed germination rate; *GI*, germination index

than the control in all tested conditions exclude the phytotoxicity factor of the produced compounds (Zhang et al. 2013). Compounds with a GI greater than 100% are considered stimulant compounds due to their ability to provide nutrients for seed germination and root growth (Wang et al. 2017; Meng et al. 2019). Therefore, all the conditions tested can be considered phytostimulants, as demonstrated by Wang et al. (2017), who composted brewery effluent with sawdust and analyzed the phytotoxicity of the compound throughout the process, finding no toxicity as early as the 12th day of processing.

Conclusion

The co-composting of green waste (GW) and biogas waste (BW) proved to be beneficial by providing complementary substrates to address the deficient characteristics of each. BW, particularly, was effective in supplying nitrogen, thereby improving the C/N ratio and facilitating a more stable and efficient composting process. Its addition enhanced the overall quality of the process by raising temperatures, balancing the C/N ratio, and ensuring optimal conditions for biological activity, ultimately leading to the stabilization of organic material in a shorter duration.

Importantly, the resulting compost from all treatments exhibited characteristics conducive to stimulating seed germination, indicating that the addition of BW did not introduce any toxicity to the mature compost. This underscores the viability and efficacy of incorporating BW into composting processes to enhance nutrient balance and overall compost quality.

Author contribution All authors contributed to the study conception and design. Material preparation, data collection and analysis were performed by Maurício Aparecido Bortoloti, Adriana Zemiani Challiol, Isabela Mangerino Sicchieri, Emília Kiyomi Kuroda, Fernando Fernandes. The first draft of the manuscript was written by Maurício Aparecido Bortoloti and all authors commented on previous versions of the manuscript. All authors read and approved the final manuscript.

Funding This work was supported by the National Council for Scientific and Technological Development of Brazil (CNPq) and carried out under the Public Call VPDE COPEL DIS 001/2017 of the Priority Project for Energy Efficiency and Strategic R&D PD2866-0472/2017, financed by Companhia Paranaense Energy—COPEL (technical-scientific cooperation contract no. 4600013405) together with the State University of Londrina (UEL).

Declarations

Ethical approval and consent to participate Not applicable.

Consent for publication Not applicable.

Competing interests The authors declare no competing interests.

References

Akyol Ç, Ince O, Ince B (2019) Crop-based composting of lignocellulosic digestates: focus on bacterial and fungal diversity. Biores Technol 288:121549. https://doi.org/10.1016/j.biortech.2019.121549

APHA, AWA, WEF (2017) Standard Methods for the Examination of Water and Wastewater, 23rd edn. American Public Health Association, American Water Works Association, Water Environment Federation, Washington, DC, p 1504

Amir S, Jouraiphy A, Meddich A, El Gharous M, Winterton P, Hafidi M (2010) Structural study of humic acids during composting of activated sludge-green waste: elemental analysis, FTIR and 13C NMR. J Hazard Mater 177(1–3):524–529. https://doi.org/10.1016/j.jhazmat.2009.12.064

Bai L, Deng Y, Li J, Ji M, Ruan W (2020) Role of the proportion of cattle manure and biogas residue on the degradation of lignocellulose and humification during composting. Biores Technol 307:122941. https://doi.org/10.1016/j.biortech.2020.122941

Bortoloti MA, Challiol AZ, Navarro BL, Sicchieri IM, Kuroda EK, Fernandes F (2023) Challenges of load variation on anaerobic digestion of organic waste on a full scale: an applied study. Waste Biomass Valorization 1–14. https://doi.org/10.1007/s12649-023-02120-9

Bustamante MA, Paredes C, Moral R, Agulló E, Pérez-Murcia MD, Abad M (2008) Composts from distillery wastes as peat substitutes for transplant production. Resour Conserv Recycl 52(5):792–799. https://doi.org/10.1016/j.resconrec.2007.11.005

Carvalho CBM, Macambira GM, Santos ACF, Oliveira HSH, da Silva DA, Ribeiro AG, Silva GD, Pessoa DV, Maciel MS, Marinho JBM, Medeiros AS, Soares GSC, Sales TB, da Silva PHF, Silva GKF (2021) Methods of analysis of chemical composition and nutritional value of feed for ruminants. Res Soc Dev 10(10):e523101019047. https://doi.org/10.33448/rsd-v10i10.19047

Chikae M, Ikeda R, Kerman K, Morita Y, Tamiya E (2006) Estimation of maturity of compost from food wastes and agro-residues by multiple regression analysis. Biores Technol 97:1979–1985. https://doi.org/10.1016/j.biortech.2005.09.026

dal Bosco TC (2017) Solid Waste Composting and Vermicomposting Academic Research Results, 1ª edn. Blucher, São Paulo, p 266

Dutta S, He M, Xiong X, Tsang DC (2021) Sustainable management and recycling of food waste anaerobic digestate: a review. Biores Technol 341:12595. https://doi.org/10.1016/j.biortech.2021.125915

El Fels L, Zamama M, El Asli A, Hafidi M (2014) Assessment of biotransformation of organic matter during co-composting of sewage sludge-lignocelullosic waste by chemical, FTIR analyses, and phytotoxicity tests. Int Biodeterior Biodegradation 87:128–137. https://doi.org/10.1016/j.ibiod.2013.09.024

El Ouaqoudi FZ, El Fels L, Lemée L, Amblès A, Hafidi M (2015) Evaluation of lignocelullose compost stability and maturity using spectroscopic (FTIR) and thermal (TGA/TDA) analysis. Ecol Eng 75:217–222. https://doi.org/10.1016/j.ecoleng.2014.12.004

Farias JS, Queiroz LO, Santos GRA, Fagundes JL, Silva MA (2015) Evaluation of fabrics and alternative equipment in the analysis of neutral detergent fibers and acid detergent fiber. Anim Ind Bull 72(3):229–233. https://doi.org/10.17523/bia.v72n3p229

Fourti O (2013) The maturity tests during the composting of municipal solid wastes. Resour Conserv Recycl 72:43–49. https://doi.org/10.1016/j.resconrec.2012.12.001

He J, Zhu N, Xu Y, Wang L, Zheng J, Li X (2022) The microbial mechanisms of enhanced humification by inoculation with Phanerochaete chrysosporium and Trichoderma longibrachiatum during biogas residues composting. Biores Technol 351:126973. https://doi.org/10.1016/j.biortech.2022.126973

Hindrichsen IK, Kreuzer M, Madsen J, Bach Knudsen KE (2006) Fiber and lignin analysis in concentrate, forage, and feces: detergent versus enzymatic-chemical method. J Dairy Sci 89(6):2168–2176. https://doi.org/10.3168/jds.S0022-0302(06)72287-1

Ho TTK, Le TH, Tran CS, Nguyen PT, Thai VN, Bui XT (2022) Compost to improve sustainable soil cultivation and crop productivity. Chem Environ Eng 6:100211. https://doi.org/10.1016/j.cscee.2022.100211

Huang D, Qin X, Xu P, Zeng G, Peng Z, Wang R, Wan J, Gong X, Xue W (2016) Composting of 4-nonylphenol-contaminated river sediment with inocula of Phanerochaete chrysosporium. Biores Technol 221:47–54. https://doi.org/10.1016/j.biortech.2016.08.104

Jimnez EI, Garcia VP (1992) Relationships between organic carbon and total organic matter in municipal solid wastes and city refuse composts. Biores Technol 41:265–272. https://doi.org/10.1016/0960-8524(92)90012-M

Jumnoodoo V, Mohee R (2011) Evaluation of FTIR spectroscopy as a maturity index for herbicide-contaminated composts. Environ Waste Manag 9:89–99. https://doi.org/10.1504/IJEWM.2012.044162

Kiehl EJ (1985) Organic fertilizers. Ceres Agronomic, Piracicaba

Kong X, Luo G, Yan B, Su N, Zeng P, Kang J, Zhang Y, Xie G (2023) Dissolved organic matter evolution can reflect the maturity of compost: insight into common composting technology and material composition. J Environ Manag 326:116747. https://doi.org/10.1016/j.jenvman.2022.116747

Li Y, Liu Y, Yong X, Wu X, Jia H, Wong JW, Zhou J (2020) Odor emission and microbial community succession during biogas residue composting covered with a molecular membrane. Biores Technol 297:122518. https://doi.org/10.1016/j.biortech.2019.122518

Liu N, Zhou J, Han L, Huang G (2017) Characterization of lignocellulosic compositions' degradation during chicken manure composting with added biochar by phospholipid fatty acid (PLFA) and correlation analysis. Sci Total Environ 586:1003–1011. https://doi.org/10.1016/j.scitotenv.2017.02.081

Maragno ES, Trombin DF, Viana E (2007) The use of sawdust in a little compounder system. Sanit Environ Eng 12(4):355–360. https://doi.org/10.1590/S1413-41522007000400001

Meng X, Liu B, Zhang H, Wu J, Yuan X, Cui Z (2019) Co-composting of the biogas residues and spent mushroom substrate: physicochemical properties and maturity assessment. Biores Technol 276:281–287. https://doi.org/10.1016/j.biortech.2018.12.097

Meng X, Yan J, Zuo B, Wang Y, Yuan X, Cui Z (2020) Full-scale of composting process of biogas residues from corn stover anaerobic digestion: physical-chemical, biology parameters and maturity indexes during whole process. Bioresour Technol 302:122742. https://doi.org/10.1016/j.biortech.2020.122742

Ofei-Quartey MNL, Appiah-Effah E, Akodwaa-Boadi K, Ampaw B, Taylor TS, Millogo ZEN (2023) Enhancing the economic potential of organic waste by co-composting using ratio modelling toward a circular economy. J Mater Cycles Waste Manag 25(3):1560–1580

Pang H, He J, Ma Y, Pan X, Zheng Y, Yu H, Nan J (2021) Enhancing volatile fatty acids production from waste activated sludge by a novel cation-exchange resin assistant strategy. J Clean Prod 278:123236. https://doi.org/10.1016/j.jclepro.2020.123236

Pramanik SK, Suja FB, Zain SM, Pramanik BK (2019) The anaerobic digestion process of biogas production from food waste: prospects and constraints. Bioresour Technol Rep 8:100310. https://doi.org/10.1016/j.biteb.2019.100310

Rueda MP, Comino F, Aranda V, Ayora-Cañada MJ, Domínguez-Vidal A (2023) Understanding the compositional changes of organic matter in torrefied olive mill pomace compost using infrared spectroscopy and chemometrics. Spectrochim Acta Part A Mol Biomol Spectrosc 293:122450. https://doi.org/10.1016/j.saa.2023.122450

Sheng X, Wang J, Cui Q, Zhang W, Zhu X (2022) A feasible biochar derived from biogas residue and its application in the efficient adsorption of tetracycline from an aqueous solution. Environ Res 207:112–175. https://doi.org/10.1016/j.envres.2021.112175

Silva ME, Lemos LT, Cunha-Queda AC, Nunes OC (2009) Co-composting of poultry manure with low quantities of carbon-rich materials. Waste Manag Res 27(2):119–128. https://doi.org/10.1177/0734242X08096693

Som MP, Lemée L, Amblès A (2009) Stability and maturity of a green waste and biowaste compost assessed on the basis of a molecular study using spectroscopy, thermal analysis, thermodesorption and thermochemolysis. Biores Technol 100(19):4404–4416. https://doi.org/10.1016/j.biortech.2009.04.019

Sun Q, Wu D, Zhang Z, Zhao Y, Xie X, Wu J, Lu Q, Wei Z (2017) Effect of cold-adapted microbial agent inoculation on enzyme activities during composting start-up at low temperature. Biores Technol 244:635–640. https://doi.org/10.1016/j.biortech.2017.08.010

Tambone F, Terruzzi L, Scaglia B, Adani F (2015) Composting of the solid fraction of digestate derived from pig slurry: biological processes and compost properties. Waste Manag 35:55–61. https://doi.org/10.1016/j.wasman.2014.10.014

Tedesco MJ, Gianello C, Bissani CA, Bohnen H, Volkweiss SJ (1995) Analysis of soil, plants and other materials. UFDS, Porto Alegre

Tiquia SM, Tama NFY, Hodgkis IJ (1996) Effects of composting on phytotoxicity of spent pig-manure sawdust litter. Environ Pollut 93(3):249–256. https://doi.org/10.1016/S0269-7491(96)00052-8

van Soest PJ (1964) Symposium on nutrition and forage and pastures: new chemical procedures for evaluating forages. J Anim Sci 23(3):838–845. https://doi.org/10.2527/jas1964.233838x

Veras RS, Stefanutti R, Lima ACA, Magalhães G (2020) Composting urban waste in static windrows with passive aeration. Mag DAE 68(224):151–165. https://doi.org/10.36659/dae.2020.047

Vig AP, Singh J, Wani SH, Dhaliwal SS (2011) Vermicomposting of tannery sludge mixed with cattle dung into valuable manure using earthworm Eisenia fetida (Savigny). Biores Technol 102(17):7941–7945. https://doi.org/10.1016/j.biortech.2011.05.056

Wang Q, Awasthi MK, Ren X, Zhao J, Li R, Wang Z, Chen H, Wang M, Zhang Z (2017) Comparison of biochar, zeolite and their mixture amendment for aiding organic matter transformation and nitrogen conservation during pig manure composting. Biores Technol 245:300–308. https://doi.org/10.1016/j.biortech.2017.08.158

Wu X, Amanze C, Wang J, Yu Z, Shen L, Wu X, Zeng W (2022) Isolation and characterization of a novel thermotolerant alkali lignin-degrading bacterium Aneurinibacillus sp. LD3 and its application in food waste composting. Chemosphere 307(3):135859. https://doi.org/10.1016/j.chemosphere.2022.135859

Xu M, Sun H, Yang M, Xie D, Sun X, Meng J, Wu C (2022) Biodrying of biogas residue through a thermophilic bacterial agent inoculation: insights into dewatering contribution and microbial mechanism. Biores Technol 355:127256. https://doi.org/10.1016/j.biortech.2022.127256

Yang WQ, Zhuo Q, Chen Q, Chen Z (2019) Effect of iron nanoparticles on passivation of cadmium in the pig manure aerobic composting process. Sci Total Environ 690:900–910. https://doi.org/10.1016/j.scitotenv.2019.07.090

Yu Z, Liu X, Zhao M, Zhao W, Liu J, Tang J, Liaoc H, Chenc Z, Zhou S (2019) Hyperthermophilic composting accelerates the humification process of sewage sludge: molecular characterization of dissolved organic matter using EEM–PARAFAC and two-dimensional correlation spectroscopy. Biores Technol 274:198–206. https://doi.org/10.1016/j.biortech.2018.11.084

Zeng G, Huang D, Huang G, Hu T, Jiang X, Feng C, Chen Y, Tang L, Liu H (2017) Composting of lead-contaminated solid waste with inocula of white-rot fungus. Biores Technol 98:320–326. https://doi.org/10.1016/j.biortech.2006.01.001

Zhang L, Sun X, Tian Y, Gong X (2013) Effects of brown sugar and calcium superphosphate on the secondary fermentation of green waste. Biores Technol 131:68–75. https://doi.org/10.1016/j.biortech.2012.10.059

Zhang T, Li H, Yan T, Shaheen SM, Niu Y, Xie S, Zhang YY, Abdelrahman H, Ali EF, Bolan NS, Rinklebe J (2023) Organic matter stabilization and phosphorus activation during vegetable waste composting: multivariate and multiscale investigation. Sci Total Environ 891:164608. https://doi.org/10.1016/j.scitotenv.2023.164608

Zhong B, An X, An W, Xiao X, Li H, Xia X, Zhang Q (2021) Effect of bioaugmentation on lignocellulose degradation and antibiotic resistance genes removal during biogas residues composting. Biores Technol 340:125742. https://doi.org/10.1016/j.biortech.2021.125742

Zhu Y, Jin Y, Liu X, Miao T, Guan Q, Yang R, Qu J (2021) Insight into interactions of heavy metals with livestock manure compost-derived dissolved organic matter using EEM-PARAFAC and 2D-FTIR-COS analyses. J Hazard Mater 420:126532. https://doi.org/10.1016/j.jhazmat.2021.126532

Zucconi F, Pera A, Forte M, Debertolli M (1981) Evaluating toxicity of immature compost. Biocycle 22:54–57